Insights into thermo-hydro-mechanical (THM) behavior of cementitious materials by means of simultaneous neutron/X-ray tomography and 3D mesoscopic modeling

Hani Cheikh Sleiman

Univ. Grenoble Alpes, CNRS, Grenoble INP, 3SR, 38000 Grenoble, France

ABSTRACT: In the last few decades, the significant advances in full-field techniques have allowed unprecedented insight into local processes. Notably, for cement-based materials, x-ray and neutron tomography lend themselves as highly complementary tools for the study of their THM behavior. In this communication, the analysis of the *in-situ* neutron tomography data-set has allowed for the quantification of the 4D moisture profiles thanks to a multiphase partitioning method applied at the voxel level. In addition, the analysis of the acquired simultaneous neutron/x-ray tomography of the cement paste sample (once aligned in time and across modalities) has allowed for the extraction of the extensive fracture network and for the estimate of its interplay with local drying. Finally, a CT-FE mapping scheme was proposed which consisted of extracting the mesoscale morphology of concrete (aggregates and pores) from x-ray/neutron attenuation fields and presenting it explicitly on a FE mesh. This has permitted to perform 3D multiphase THM simulation of concrete at the mesoscale.

Keywords: X-ray tomography, Neutron tomography, THM behavior, 3D mesoscopic modelling

1. Introduction

The durability and structural serviceability of cement-based materials are major concerns in civil engineering due to their significant economic, social and environmental repercussions. Drying plays a central role in this, given that the changes in saturation of the pore network, together with the associated drying shrinkage are leading processes in the cracking and the penetration of aggressive chemicals in the material. The conventional experimental techniques such as gravimetric and sensor-based measurements, which are employed to study the drying-driven processes, provide only bulk-averaged or point-wise measurements which are not sufficient to characterize these intrinsically heterogeneous processes. However, the significant advances in full-field techniques have allowed unprecedented insight into these local processes **[Viggiani and Tengattini, 2019]**. Notably, for cement-based materials, x-ray and neutron tomography lend themselves as highly complementary tools for the study of their THM behavior. In fact, the high sensitivity to density variations of X-ray imaging gives access to the developments of fractures, in 4D (3D+time). On the other hand, neutron tomography allows the study of the evolution of the moisture field in 4D, thanks to its high hydrogen sensitivity.

On the flip side, the numerical models, which were developed in last few years, have shown a strong potential in simulating the mass, energy and momentum transfers in cement-based porous

media subjected to THM loading. However, these models' simulations were only validated against bulk-averaged macroscopic measurements but no clear strategy was yet proposed to validate the models' predictions of the local processes taking place at the mesoscale.

This paper highlights the contribution of neutron and X-ray tomography in characterizing the thermo-hydro-mechanical behavior of cement-based materials. Particularly, the 5D tomographic study herein focused on characterizing the moisture transport and cracking local effect in a cement paste sample and a concrete one that were subjected to moderate temperature gradients. In addition, the complementary imaging data-sets were used to feed a well-established multiphase numerical model with morphological information. This has been done thanks to a CT-FE mapping scheme that extracted the aggregates and pore (captured respectively by neutron and X-ray 3D images) and projected their morphologies on a FE mesh. The proposed method allows for 3D multiphase simulations of the THM behavior at the mesoscale and allows for a consistent comparison ground of the imaging-based full-field measurements.

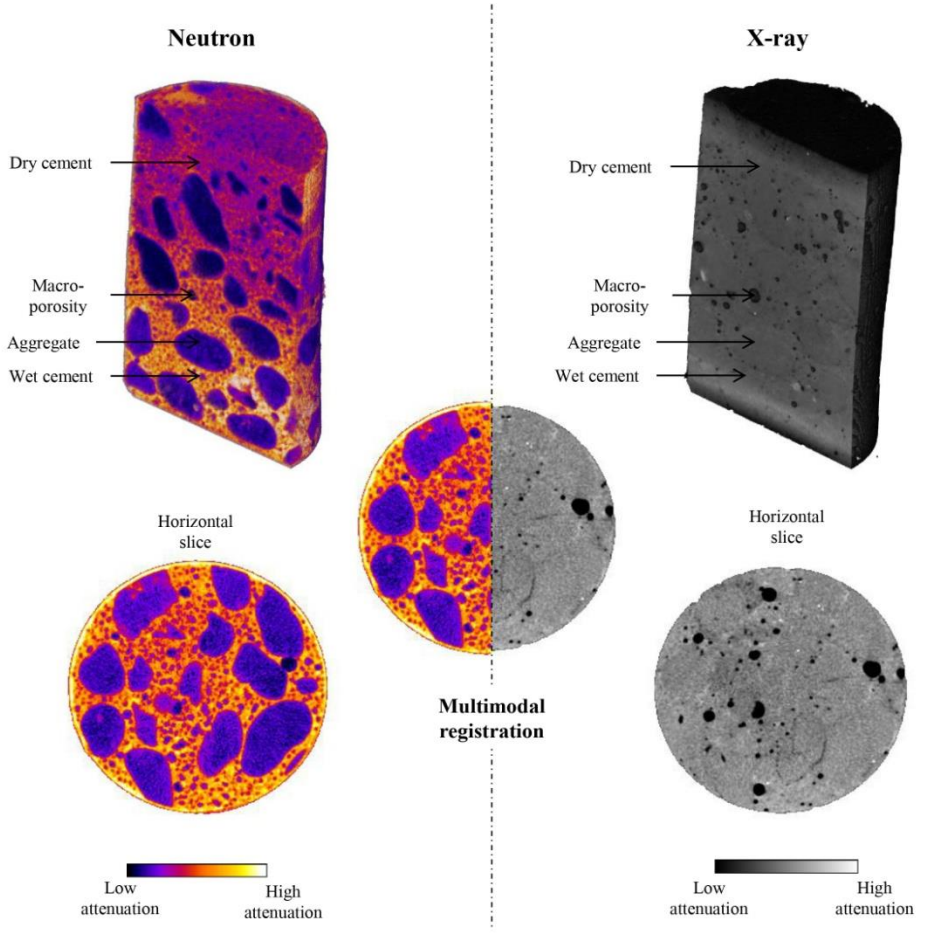

FIGURE 1. Vertical and horizontal slices of the 3D reconstructions of the neutron and X-ray tomographies of the concrete sample, highlighting the high complementary of the micro-structural information obtained with these techniques. The neutron attenuation field (the average attenuation of the materials contained in a voxel μ_n) on the left of the partially saturated concrete sample highlights aggregates and pores from the cement paste which is further differentiated in dry and wet. Nonetheless pores and aggregates have comparable attenuation in the neutron tomography whereas they have significantly different X-ray attenuations μ_x, as shown on the right.

2. *in-situ* simultaneous neutron/X-ray tomography

2.1. Materials and methods

- **Heating setup**

The designed cell has a principal functionality of heating the samples on their top surface, from which the moisture is extracted. Its materials were chosen to be as transparent as possible to both neutrons and X-ray, while the design was chosen to minimize the sample to detector distance and therefore to maximize the resolution output. Figure 2 (top left) illustrates the different components of the cell. The temperature of the radiator is servo-controlled thanks to a built-in thermocouple connected to regulator which allows for temperature modifications during the test.

- **Tested samples**

Two samples were tested during this experimental campaign: a concrete one and a cement paste one. The former was cored out from a R30A7 concrete bloc while the later, having a water-to-cement-ratio of 0.5, was cast in a commercial plastic mold. Just before testing, the samples were wrapped in three layers of self-adhesive aluminum tape (aluminum being particularly neutron transparent), to minimise moisture escape from the lateral surfaces during the test, and therefore to induce a unidirectional moisture flow. The samples were also equipped with a type K thermocouples that were placed at the top of the sample to measure its surface temperature.

- **Neutron and X-ray tomography acquisitions**

The X-ray and neutron tomographies were acquired at the NeXT-Grenoble beamline (detailed in **[Tengattini et al., 2020]**. Two slightly different sets of parameters were employed in the two tests on concrete and cement, respectively, each optimised for the expected speed of the processes.

For the concrete sample, the parameters were optimised to achieve simultaneous acquisitions every 7 minutes. Specifically, 900 projections were acquired over a 360^o rotation. Each neutron radiography was average over two acquisitions each with a 0.2s exposure. These parameters, together with a suitable choice of the scintillator type and the pinhole diameter, yielded a resolution just above 100 microns. For the X-ray, the generator was set at 130V and 230A, which allowed the acquisitions of 9 frames per second, each of which was then averaged over 4 projections, acquired fully simultaneously to the neutron tomographies.

For the cement paste test, the parameters were optimised to achieve simultaneous acquisitions every 30 minutes. Specifically, 1200 projections were acquired over 30 minutes for a 360^o rotation. Each neutron radiography was the average of 3 individual projections each with a 0.5s exposure. 1200 projections were acquired for a 360^o rotation. The neutron resolution attained was about 75 microns. The X-ray source was maintained at 130V and 230A, and the flat panel was set still at its maximum speed of 9 frames per second, but to maintain the 30 minutes of the simultaneous tomography, each radiography was the average of 13 individual acquisitions.

These sets of radiographies were reconstructed into the corresponding 3D volumes by means of the Feldkamp (FDK) back projection algorithm, as implemented in the commercial software X-act (from RX-Solutions). An example of the 3D neutron and X-ray attenuation fields are reported in Figure 1 for the concrete sample.

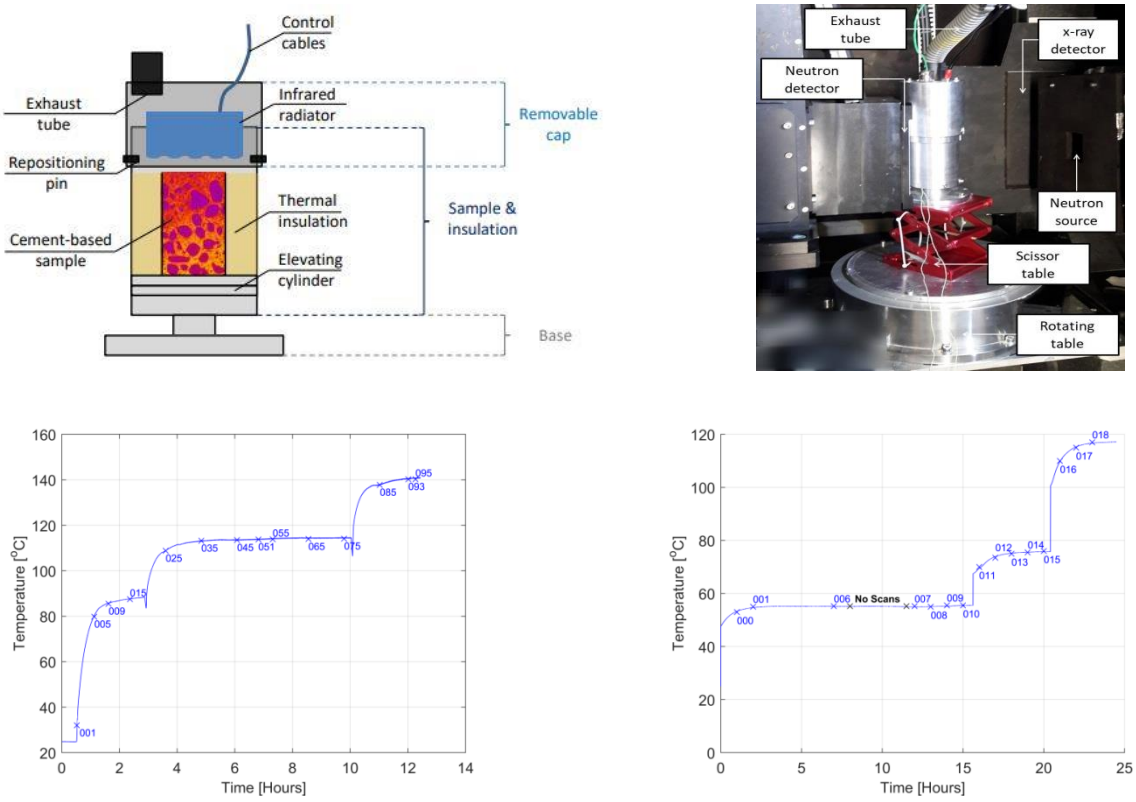

FIGURE 2. (Top left) Schematic view of the heating setup highlighting the positions of the sample wrapped with aluminum tape for moisture isolation and rockwool for heat isolation, the exhaust output and the infrared radiator. (Top right) Heating cell in beam-line (X-ray source yet to be moved): the cell is to be crossed by a neutron flux on a first axis and by an X-ray flux on a nearly-perpendicular second axis. (Bottom) Measured temperature on the top surface of the tested concrete sample (bottom left) and of the cement paste sample (bottom right).

- **Thermal testing conditions**

In both tests, the temperature of the radiator was servo-controlled. Given the air gap of few millimeters between radiator and sample, there is a slight discrepancy between the imposed temperature and the one at the top of the sample, which was measured thanks to the thermo-couple installed on its top surface. The heating temperature and duration were estimated based on preliminary numerical and experimental analyses and were adapted during the tests based on the observed results. Figure 2 (bottom) illustrates the temperature history measured on the top of the concrete sample (bottom left) and cement paste sample (bottom right). Multiple tomography stamps were added to this plot to indicate important time instances at which some of the relevant simultaneous N/X tomographies were acquired.

2.2. Results

- **Concrete sample**:

Moisture transport in concrete happens essentially in the cement paste porosity and in the macro-porosity, given that aggregates and sand grains are comparatively impermeable. In order to characterize fluid transport, the aggregates and the sand particles should not be considered in the analysis. The aggregates, easily detectable in the images, were therefore isolated and removed from

all ensuing analyses. This operation is relatively straightforward giving their distinct attenuation in the neutron tomographies, lower than that of the cement paste, which can be used to identify them (a process named segmentation). To better assess the quality of this segmentation as well as to better understand the minimum grain size removed with this technique, a granulometric analysis was also performed. This consists in separating the segmented image into the individual grains (applying a morphological operation named "watershed". The probability density function of these grain sizes is compared against experimental sieving measurements provided in **[Vu, 2007]**. It is worth mentioning all fines having an average diameter lower than 800 microns (corresponding to 6 to 7 pixels) were not captured by segmentation due to resolution limitations. After registering all the neutron volumes and segmenting the reference neutron image, the average gray level attenuation of the remaining mortar along the height of the sample is calculated for each volume. At the beginning of the test, the gray value profiles indicate a mostly homogeneous water distribution along the sample. As the temperature in the sample increases, the drying process starts affecting predominantly the top of the sample. As the test progresses further, more of the sample undergoes water loss, and the gray value gradient is nearly linear along most of sample height. Eventually, the top 1.5 cm of the sample reaches an asymptotic value corresponding presumably to the hydric equilibrium. On the other hand, it is important to understand how water loss is related to the attenuation of the mixture. Once the aggregates are removed by segmentation, the attenuation of the remaining mortar voxels is the combination of the attenuation of three "species": air , water and dry mortar. Specifically, the attenuation coefficient μ is the summation of the individual contributions of the species composing it, weighted by their volumetric fraction W, which can be expressed as:

$$\mu_{mix} = W_{dm}\mu_{dm} + W_w\mu_w + W_a\mu_a \quad (1)$$

This has permitted to estimate the variation of the volume fraction of water in the mortar matrix as illustrated in figure 4 (right). Furthermore, the 20% estimation of water volume fraction loss is coherent with the granulometric analysis prediction of the mortar porosity (estimated by 26%).

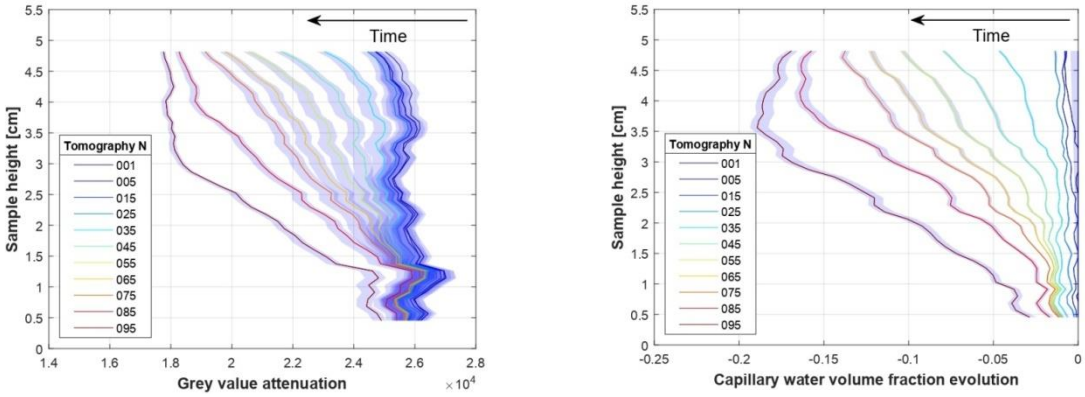

FIGURE 3. (Left) Gray value attenuation gradient evolution along the sample height, (Right) Capillary water volume fraction evolution along the sample height. The transition from gray value to water volume fraction was done thanks to a multiphase partitioning at the voxel level.

- **Cement paste sample**:

The cement paste sample has shown cracking initiation and its propagation along the test as highlighted in Figure 4 (Top Left). The cracks initially appear on the outer surface, and

predominantly in the warmer top section of the sample. Once the fracture network has been isolated it is possible to assess its effect on drying thanks to the complementary neutron dataset. In order to do this, a 5D volume registration is pivotal to ensure that each voxel represents the same volume in space across time and modalities as seen in Figure 4 (Bottom Left). Then, it is relatively straightforward to study the effect of the cracks on water content by studying the evolving gray value in the neutron dataset in the vicinity of the cracks. From a technical standpoint, it is possible to identify the areas neighbouring a fracture by dilating the binary image of the cracks multiple time (Figure 4 Left).

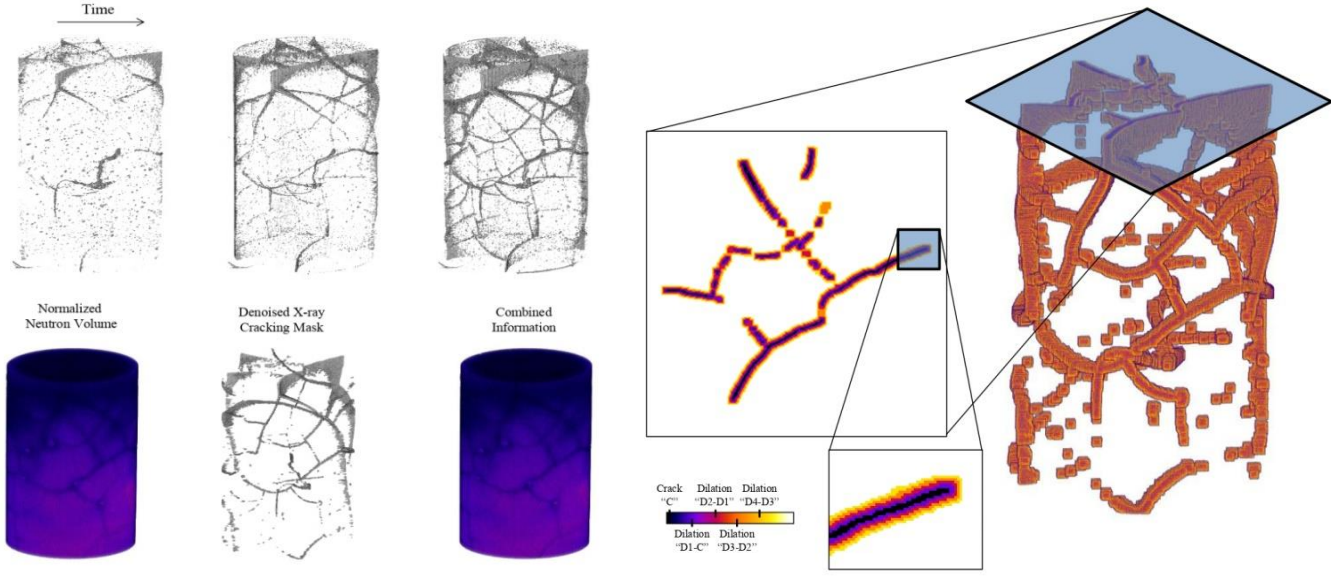

FIGURE 4. **(Top Left) Cracks initiation and propagation in time extracted from X-ray tomography: (left) 007, (middle) 012, (right) 017; (Bottom Left) 3D visualisation of cracks and neutron images after multimodal registration : normalized neutron volume (left), 3D denoised X-ray cracks (middle) and combined images (right); (Right) Crack dilation procedure.**

No gradients were measured in the top part of the sample due to the rapid occurrence of drying. However, in the middle and bottom it can be observe that drying starts predominantly near fracture and progressively propagates outwards as the overall drying progresses. This analysis suggest that the effect of the fracture can go as far as 4 mm away from it.

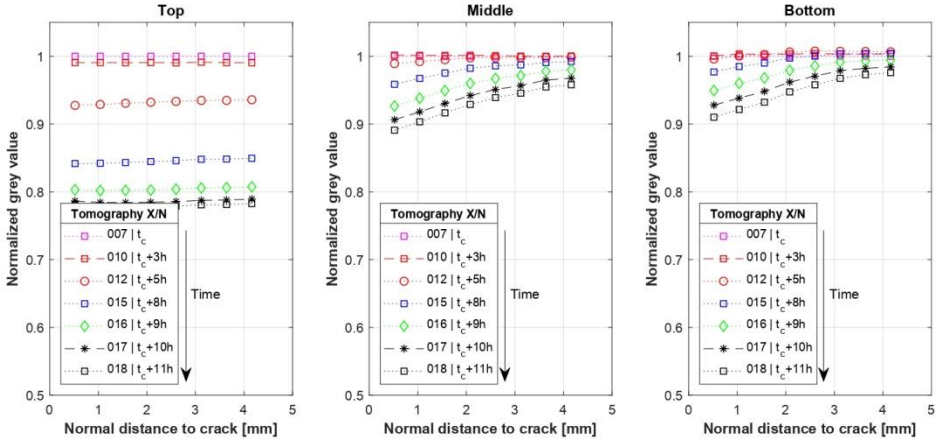

FIGURE 5. **Evolution of cracking local effect on the water content in the normal direction to the crack.**

3. 3D image-based multiphase modeling of concrete at the mesoscale

In this section, concrete is modeled as a multiphase porous material that comprises a solid skeleton and a pore network having liquid water, vapor and dry air. The numerical model is based on the hybrid mixture theory in the mathematical formulations proposed in **[Lewis and Schrefler, 1998]**.

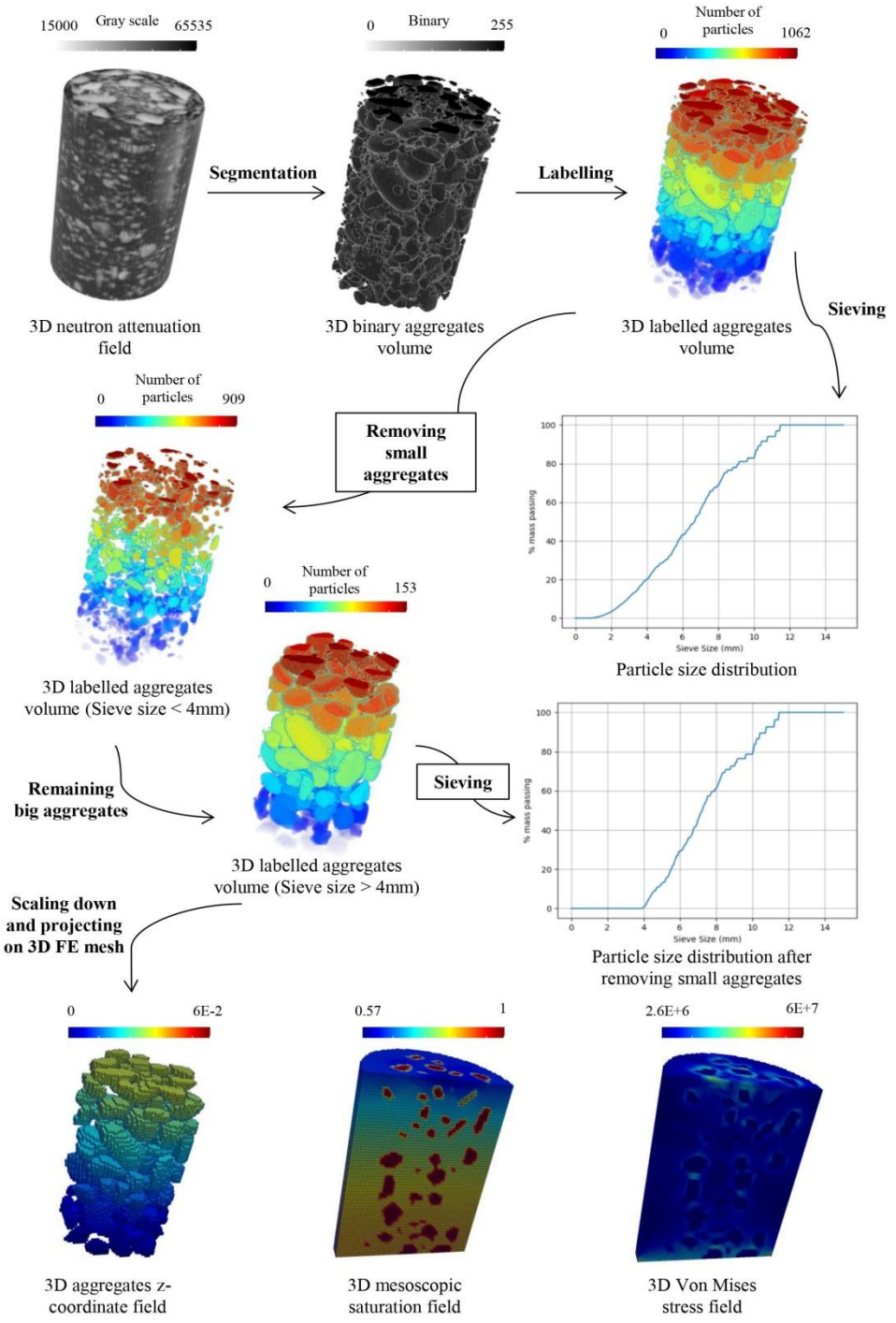

FIGURE 6. CT-FE mapping scheme to perform 3D THM simulation of concrete at the mesoscale while representing the aggregates real morphology

We propose herein a CT-FE mapping scheme that extracts the mesoscale morphology of concrete (aggregates and pores) from X-ray/neutron attenuation fields and presents it explicitly on a FE mesh. The full procedure is illustrated in Figure 6, it consists on: segmenting of the initial 3D neutron attenuation field to isolate the aggregates; separating and labeling of the aggregates by means of a watershed algorithm; manipulating the meso-structure by removing the aggregates and sand particles having a diameter below a certain threshold (optional); scaling-down the image to reduce the numerical model's computational time cost since each voxel in the image represents a finite element in the mesh; projecting the morphology on the finite element mesh using a developed procedure in Cast3m FE software; Assigning the input parameters, models and boundary conditions of the two different materials to simulate the THM problem; Post-processing the results which requires additional scripts development in order to extract the nodal quantities which belong to the mesh of the mortar specie or to some local region in the material for instance. The proposed method allows for 3D multiphase simulations of the THM behavior at the mesoscale and allows for a consistent comparison ground of the imaging-based full-field measurements.

4. Conclusion

Simultaneous neutron and X-ray tomography were acquired for a concrete and a cement paste samples submitted to drying under moderate temperature. Multiple image processing were proposed in order to quantify local processes in those cement-based materials. Specifically, a multiphase partitioning method was proposed for the concrete sample to transition in between grey value and liquid water saturation. This has allowed to quantify the evolution of saturation gradients along the sample's height. The analysis has shown an overall loss of 20% volume fraction of water which was found to be below 26% of the porosity volume fraction (estimated from particle size distribution). For the cement paste sample, the proposed image analysis has permitted to quantify for the effect of the cracks on the local drying. Many steps were required in order to achieve this quantification, perhaps the most prominent ones were the cracking extraction, the multimodal registration and the cracking dilation procedures. The analysis has shown that the cracking might induce local drying gradients that can reach as far as 4 mm in its vicinity. Finally, a CT-FE mapping scheme was proposed which allows for 3D mesoscale FE simulations by projecting the concrete meso-morphology explicitly on the FE mesh.

REFERENCES

[Viggiani and Tengattini, 2019] Viggiani, G. and Tengattini, A., 2019. Recent developments in laboratory testing of geomaterials with emphasis on imaging, Proceedings of the XVII ECSMGE-2019, doi 10.32075/17ECSMGE-2019-1112.

[Tengattini et al., 2020] Tengattini, A. and Lenoir, N. and Andò, E. and Giroud, B. and Atkins, D. and Beaucour, J. and Viggiani, G., 2020. NeXT-Grenoble, the neutron and X-ray tomograph in Grenoble, Nuclear Instruments and Methods in Physics Research Section A: Accelerators, Spectrometers, Detectors and Associated Equipment, 163939

[Vu, 2007] Vu, X. H., 2007. Caractérisation expérimentale du béton sous fort confinement : influences du degré de saturation et du rapport eau/ciment, Université Joseph Fourrier.

[Lewis and Schrefler, 1998] Lewis, R. and Schrefler, B., 1998. The Finite Element Method in the Static and Dynamic Deformation and Consolidation of Porous Media, John Wiley.